Modelling Programmable Deformation of Particle-Based Structure with Smart Hydrogels

Chen, Qianyi; Kalpoe, Tarish; Jovanova, Jovana

DOI
10.1109/ReMAR61031.2024.10617511

Publication date
2024

Document Version
Final published version

Published in
Proceedings of the 6th International Conference on Reconfigurable Mechanisms and Robots, ReMAR 2024

2024 6th International Conference on Reconfigurable
Mechanisms and Robots (ReMAR)
June 24-27, 2024. Chicago, IL, USA

Modelling Programmable Deformation of Particle-based Structure with Smart Hydrogels

Qianyi Chen[a*],Tarish Kalpoe[a], Jovana Jovanova[a]

2024 6th International Conference on Reconfigurable Mechanisms and Robots (ReMAR) | 979-8-3503-9596-9/24/$31.00 ©2024 IEEE | DOI: 10.1109/REMAR61031.2024.10617511

***Abstract*— Grippers are widely used in many industrial applications, but are limited due to their rigid constructions and no adaptability to varying stiffness. The solution for this would be the use of soft grippers. One way to design soft grippers is to use smart materials, such as hydrogels. Hydrogel soft grippers, unlike their rigid counterparts, take advantage of smart materials' inherent responsiveness and adaptability, removing the need for external power components. To explore the possibilities of using smart hydrogel as the actuator in the soft gripper, we proposed a bilayer structure including temperature sensitive hydrogel and silicone. In order to get insight into the design of these configurations for a gripper, a model consisting of hydrogel was proposed to execute simulations using Finite Element Method (FEM) in Abaqus. The results show, that by modelling different configurations with temperature as input, information can be obtained about mechanical properties such as expansion and bending. Moreover, various forms of deformation can be attained through the utilization of programmable configurations. These configurations can be tailored to achieve deformations in diverse scenarios, including bulk material conveying or underwater applications.**

***Keywords*–Smart materials, Temperature-sensitive hydrogel, Soft gripper, Modelling, FEM**

I. INTRODUCTION

In many industrial applications the use of grippers is needed [1]. However, this can be very challenging depending on its application. Applications involving grasping of objects which are fragile or have an arbitrary shape are particularly difficult. Unfortunately, most current applications experience limitations due to rigid constructions and no adaptability to the stiffness or shape of the objects to be grasped. Typical machines or robots using grippers consist of materials which are rigid and limit the capability of the gripper to adapt to different shapes or stiffness [2]. The solution for this would be to make use of a soft gripper, which has the option to adapt to the irregular shapes of objects [3]. Studies performed in the past, argue that soft grippers perform well in grabbing irregular-shaped objects [1]. Furthermore, some control tasks such as closing or opening of the gripper's fingers, which are given to a rigid gripper can now be carried out by the mechanical properties of the soft gripper itself [4]. One way to assemble soft grippers is to make use of smart materials as a base for the skeleton [5]. Smart materials can have a change in shape as a response to certain external stimuli, such as light or temperature [6]. They are mostly inspired by nature in contrast to hard materials used in engineering. The materials can be classified into specific types, such as gels, dielectric elastomers and shape memory polymers [7]. A specific type of gel, hydrogel, shows the most potential of all smart materials because of their wide applicability. The advantage of hydrogel is that certain material parameters can be changed. Due to external stimuli caused by for example temperature changes, the material can increase and decrease in size [8]. Due to these stimuli, different configurations could be obtained by controlling the expansion or shrinkage of hydrogel. By having this property one could 'program' the structure by making use of granular materials, in this case, hydrogel particles. By adding silicone to hold these hydrogel particles together, configurations could be achieved to make the hydrogel particles function as an adaptable skeleton for a gripper. It is worth noting that the focus is being placed on the expansion since shrinkage is not needed for the concepts explored. This study developed a novel actuation method based on smart materials that can be used to design and fabricate soft grippers. First, a subroutine model has been developed to describe the active behaviours of hydrogel. Secondly, different actuating configurations consisting of a combination of hydrogel and silicone particles were proposed. Lastly, the proposed configurations were simulated to explore the potential applications in soft grippers based on smart materials.

II. METHODOLOGY

A. Hydrogel properties

Many are accustomed to using gels in food and beauty products, such as paints or fillers. However, gel has been mostly used for drug-delivery or soft actuators [9]. Therefore, there has not been much research on hydrogel being applied as a gripper with different geometries. Research performed was mostly focused on grippers with layers of bending strips [10]. Hydrogel is the main component of this study, more reason to establish the parameters and characteristics associated with this material. Hydrogel is a gel type which gets swollen by water absorption. It is a soft active material which shows volume changes as a response to a variant of external stimuli such as temperature, concentration, light, etc. [11]. By combining the soft hydrogel (active material), with for instance passive hard materials a smart system can be created. In this case passive is defined as a material which is not actively stimulated. By combining both materials one can use the advantages of each material type in a structure. The soft material makes the system smart and simple to deform, while the hard material provides the needed stiffness and ensures the structural capabilities. The temperature-sensitive hydrogel poly(N-isopropylacrylamide), also known

[a]Department of Maritime and Transport Technology Faculty of Mechanical Engineering, Delft University of Technology, 2628 CD Delft, The Netherlands * Q.Chen-5@tudelft.nl

as PNIPAM, has garnered considerable interest in the family of stimulus-responsive hydrogels due to its distinctive properties, including ease of production, tuneability, and good integrability [6].

B. Hydrogel expansion

Hydrogel is a hyperelastic material, meaning that it has non-linear behaviour. To determine the expansion the non-linear field theory of coupled diffusion and deformation needs to be adapted [12-16]. These equations are based on PNIPAM modelling [6]. This results in the free energy being:

$$W\left(I_1, I_3, \mu, T\right) = \frac{1}{2} N k_{\mathrm{B}} T \left(I_1 - 3 - 2\log I_3\right) - \frac{k_{\mathrm{B}} T}{v}\left[\left(I_3 - 1\right)\log\frac{I_3}{I_3 - 1} + \frac{\chi\left(T, I_3\right)}{I_3}\right] - \frac{\mu}{v}\left(I_3 - 1\right), \tag{1}$$

with I_1 and I_3 being the first and third deformation gradient tensors. N is the number of chains per volume of the polymer, T is the temperature, μ is the chemical potential, v is the volume of a solvent molecule and k_B is the Boltzmann constant. The equations consist of the elastic energy, mixing energy and work done by the chemical potential, making the equation consist of three parts. This also makes use of the Flory-Huggins interaction parameter χ, and this can measure the enthalpy of the mixing process as a function of T for the hydrogel which is temperature-sensitive:

$$\chi(T, I_3) = A - 0 + B_0 T + (A_1 + B_1 T)/I_3. \tag{2}$$

The coefficients A_i and B_i are determined by experiments on PNINAM hydrogels [17]. By having Equation 2 the components can be computed for the first Piola-Kirchhoff stress, **P**, which is shown here:

$$\mathbf{P} = \frac{\partial W_0\left(I_1, I_3\right)}{\partial \mathbf{F}} = \frac{\partial W_0\left(I_1, I_3\right)}{\partial I_1}\frac{\partial I_1}{\partial \mathbf{F}} + \frac{\partial W_0\left(I_1, I_3\right)}{\partial I_3}\frac{\partial I_3}{\partial \mathbf{F}}. \tag{3}$$

This equation was further used to solve the other stress tensors and resulted in the computation of deformations.

For the modelling of hydrogel particles, the simulation will be set up in the program Abaqus [18]. This software can be used to determine the expansion and thus the deformation of the different hydrogel configurations. The properties of hydrogel are not part of the tools in Abaqus, therefore as mentioned before the user-defined hyperelastic material subroutine needs to be used to run the simulations [6]. The above-mentioned equations and coefficients were included in a subroutine which was used in the modelling tool. It is worth noting that due to the hydrogel being non-linear, a Neo-Hookean input is needed in the material library. This depends on three inputs: the initial swelling ratio (λ_0 = 1.5), the equilibrium chemical potential ($\mu = -0.0343$) and the dimensionless parameter (Nv = 0.01) which indicates the crosslink density.

III. MODELLING APPROACH

A. Actuation method

The actuating method mentioned earlier is based on the concept of having two layers connected each having different material properties. One layer consists of hydrogel and one layer of silicone. By decreasing the temperature, the hydrogel would expand, while the silicone would stay the same size. This difference in behaviour leads to the bending deformation of the entire structure. Therefore, making the structure function as an actuator with temperature as the stimulus. The design is based on the examples given in [19] and [20], with the desired deformation mode being bending.

B. Simulation setup

Abaqus was used to simulate the hydrogel particles. During this research, the version used is Abaqus CAE (Complete Abaqus Environment), which enables one to create, monitor and visualise advanced Abaqus analyses quickly.

1) Material and geometry: Two material types were simulated, the hydrogel (PNIPAM) and the silicone (ecoflex 00-10) which functioned as the structure for the hydrogel particles [21]. Both of these materials were modelled as spheres, each with a diameter of 20 mm. All the configurations have been designed with hydrogel as ideal spheres, in reality, this will not always be the case and be harder to obtain. However, for the proof of concept of the actuation method, this is currently sufficient. To ensure that these balls stay fixed together, a bit of overlap (1 mm) was introduced. A schematic depiction of the front view of the geometry of multiple particles with the overlap is given in Fig. 1a. In this figure the green particles indicate silicone and the light grey particles are hydrogel, this distinction will be used with other configurations as well. An isometric view of a merged geometry in Abaqus is also given in Fig. 1b.

(a) Schematic front view (b) Isometric view

Fig. 1: Initial configuration of the combined hydrogel and silicone part

2) Mesh: All the particles in this setup are meshed with the C3D8H element [22]. The global mesh size used was 0.5 mm, this was chosen to ensure that the mesh fitted the round edges, since the particle geometry only contains spheres.

3) Timesteps: The simulation used timesteps to accurately calculate the expansion of the hydrogel particles and the deformation of the entire structure. This was performed with a static general model. For each timestep, a predefined field was created with a different temperature. In this case, the objects were cooled, thus several fields were created, each with a lower temperature. The initial temperature was set at 300 K and was decreased in steps of 5 K until a

final temperature of 275 K was reached. By doing this, five additional steps were created with their corresponding temperatures.

4) Boundary conditions: Due to the goal being the observation of the deformation of the particles as a result of expansion, other forces were deemed irrelevant within the scope of this research. The only boundary condition added was a fixed constraint on one corner silicone ball for almost every configuration. The reason for this was to ensure that the part did not float around in the simulation space due to the expansion. This constraint is also schematically indicated in Fig. 1a with a blue triangle and was also applied for every configuration in this section.

C. Configurations

1) Reference case-C1: The configuration uses particles which are 40 times bigger than the one mentioned in the example of the paper [20], but the design setup is the same. The referenced configuration consisted of five balls of each material type in a row. Two of these rows were placed on top of each other, forming a configuration with ten balls. Each row had its specific polymer properties depending on the material being silicon or hydrogel. The purpose of this configuration was to obtain bending around the Z-axis. For further analysis, the number of particles used in the reference case was increased, these configurations were labelled under the first configuration (C1). Thus extending the configuration with a hydrogel ball and silicon ball. The reason for this was to obtain a larger curved area. The goal was to find out how many particles were needed to obtain a circle and how the elongation of the configuration would influence the bending between particles. The schematic 2D depiction of the configuration with the respective 'fix' constraint can be found in Fig. 2a. In Fig. 2b an example is given of 20 balls, with the red rectangle indicating a 'ball pair'.

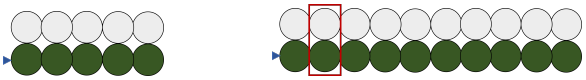

(a) The reference case (b) C1 with ten pairs

Fig. 2: C1 configurations

2) C2: The second configuration consisted of twice the initial configuration and a reversal of the material type in the middle. This could have resulted in alternations between the orientations. An example is given here, with 20 balls as shown in Fig. 3a. With this, an 'S' shape could be obtained by bending in two directions for each five ball pairs. This would have been useful for an object with a varying width. In addition to this, alternative options to this configuration were made. One of these is showcased in Fig. 3b.

3) C3: The first of the combined combinations made use of configuration 2 with the extension of a multipair of configuration 1, which can be seen in Fig. 4a. The configuration consisted of 32 particles in total, with again having a 1:1 ratio between hydrogel and silicone. The reason for this combined configuration was to explore if a 'hook' or

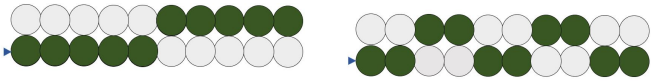

(a) Configuration 2a (b) Configuration 2b

Fig. 3: Schematic overviews C2

'tentacle' could be formed, by first initiating bending in two opposite orientations and following with a longer segment of the same ballpairs in the end. The isometric view of this configuration is given in Fig. 4a.

4) C4: The last configuration was a combination of two configurations perpendicular to each other as can be seen in Fig. 4b. The setup consisted of 37 hydrogel and 37 silicone particles. Since this gave the finger enough particles to curl towards each other, to confine a sphere. In addition to this, a single particle was needed to be at the centre to place a fixed constraint. All of this resulted in two crosses of 36 particles with a particle pair in the centre, leading to 74 particles in total. This was the first configuration that could function as a gripper. In this case, the middle silicone ball was fixed (indicated in red) and would function as the centre for the entire configuration. This would result in the fingers curling towards the centre.

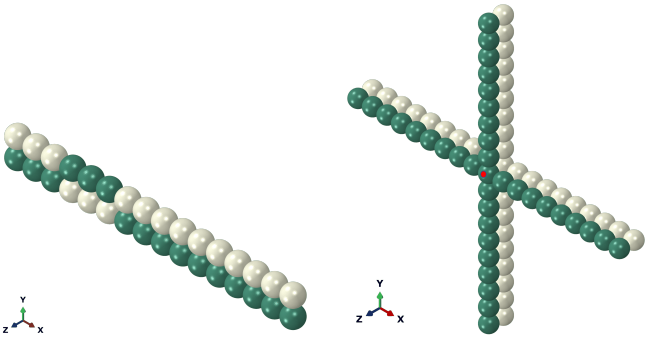

(a) C3: 'The hook' (b) C4: 'The gripper'

Fig. 4: Isometric view of the combined configurations

IV. RESULTS AND DISCUSSION

A. Verification of the PNIPAM hydrogel

1) Single hydrogel ball and first pair: The first simulation yielded the expansion of one single hydrogel ball with a temperature decrease from 300 K to 275 K. The expansion given below in Table I is expressed in the diameter ratio and volume ratio.

TABLE I: Expansion single hydrogel ball

T [K]	**D** $[mm]$	D/D_0 [-]	V/V_0 [-]
300	20.00	1.00	1.00
295	22.84	1.14	1.50
290	24.44	1.22	1.82
285	25.65	1.28	2.11
280	26.62	1.33	2.36
275	27.45	1.37	2.59

To investigate the expansion rate a plot has been made with the diameter as a function of time as can be seen in Fig. 5. Each red dot represents the final temperature reached at the end of a time step. In this plot, the data points show a decreasing expansion rate. The expansion slows down with each timestep as the temperature decreases. By looking at the function, a logarithmic curve can be observed.

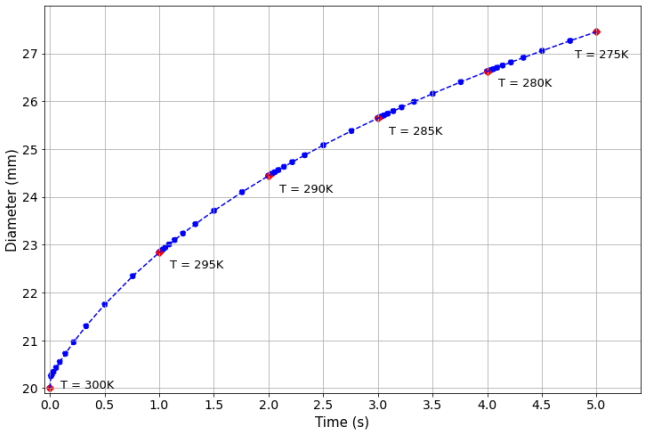

Fig. 5: Expansion plotted against the time

2) First configuration - reference case: With lowering the temperature, bending can be observed along the five ball pairs. In Fig. 6 the final state of the configuration can be found. The corresponding bending angle, ϕ between the outer pairs at the final step of each of the five temperatures has been obtained. This bending angle and the corresponding difference in angle, $\Delta\phi$, between each temperature can be found in Table II. It should be noted that the given bending angle depends on the configuration. The specific angle, ϕ*, can be determined with Equation 4. In this case, n is the number of ball pairs. This is a more accurate representation since the bending angle would be greater if the chain of ball pairs were extended. Furthermore, it is important to note that the proposed configuration has been verified by earlier research [19].

$$\phi* = \frac{\phi}{n-1} \tag{4}$$

TABLE II: Bending angles and differences reference case

T [K]	ϕ [deg]	$\Delta\phi$ [deg]	ϕ* [deg]	$\Delta\phi$* [deg]
300	0	0	0	0
295	28.1	28.1	7.03	7.03
290	41.1	13.0	10.29	3.26
285	52.2	11.1	13.05	2.76
280	59.8	7.6	14.95	1.90
275	65.7	5.9	16.43	1.48

B. Effect of different design parameters

1) C1 - Multipair: Here the results of the multipair simulations can be found. The simulation of the setup used had been performed with 20, 26, 32, 40 and 44 balls. It must be stated that by estimations, it was found that 44 is the minimum to reach a full circle with the given set-up. Therefore, the last simulation of 44 balls has specifically been chosen. The deformation at the final temperature for various cases can be seen in Fig. 7 respectively. As can be seen, the type of deformation is not influenced by the amount of particles. The same curling behaviour can be observed in both cases. The radius in each case between the centre of the curl and the particles does not differ.

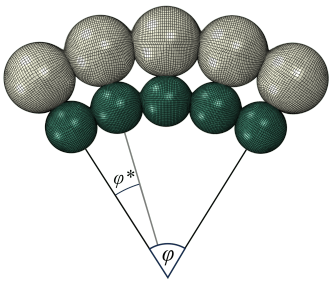

Fig. 6: Reference case at T = 275 K

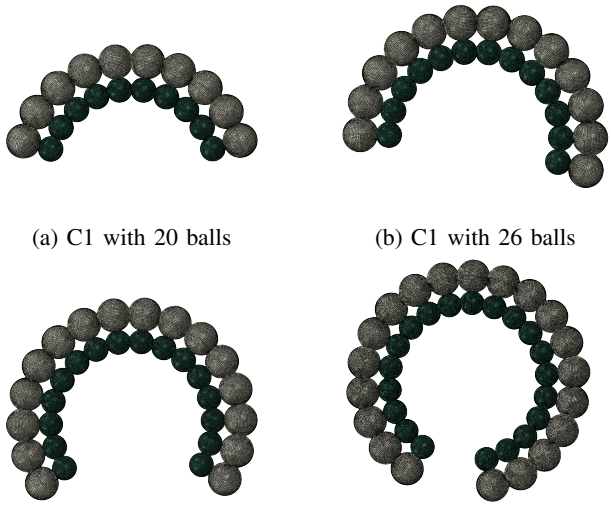

(a) C1 with 20 balls (b) C1 with 26 balls

(c) C1 with 32 balls (d) C1 with 40 balls

Fig. 7: Results multipair simulations at T = 275K

Important to note is that the simulation did not account for interactions. For example, by looking at Fig. 8, one could assume that a perfect circle had been formed with the 44 balls. However, by zooming in this is not the case. In the zoom-in of the figure, a clear connection between both ends can be found, with this connection having a bigger overlap than the neighbouring overlaps. Two circles with the same diameter have been placed at the connecting point to highlight the difference in overlap. Meaning that this is not a perfect circle and the particles were moving in one another due to the lack of interaction constraints. In reality, the particles would push against one another. It is important to note that the amount 44 is the minimum needed to obtain the circle, any amount lower than this will leave a considerable gap in between the particles.

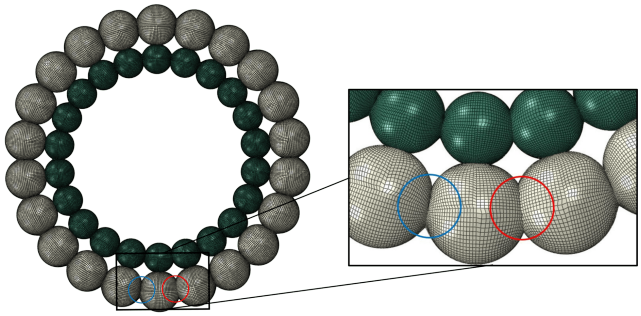

Fig. 8: C1 with 44 balls at T = 275 K

One aspect that continued to show is the influence of the boundary condition, in this case, the 'fix' constraint placed on the silicone ball. This fixed constraint functions as a hinge in every direction, which can be observed in Fig. 13. The hinge point only influences the orientation but not the deformation. Secondly, it can be noticed that with larger configurations, out-of-the-plane rotations can also be observed. Almost all the longer configurations have been slightly rotated out of the X-Y plane. Most of the configurations were made in the X-Y plane and are deformed and bent in this plane. However, the longer configurations tended to rotate around the fixed silicone ball in the Z-direction. This can be seen in Fig. 9 for the C1 with 32 balls. Rotation around the X-axis and Y-axis can be found. A vertical and horizontal axis have been drawn with dotted lines to indicate the angle made with the axis. Even though these rotations seem to be small, this could influence the determined bending angle, since this was done by looking at the X-Y plane. For the next step, the intention is to delve deeper into the interaction dynamics between silicone and hydrogels, aiming to enhance stabilizing the entirety of the structure.

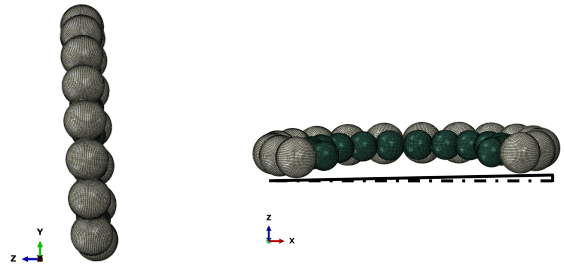

(a) Z-Y view (b) Z-X view

Fig. 9: Out of plane rotations - 32 balls at T = 275 K

The specific bending angles for the four configurations mentioned earlier and the reference case, consisting of ten balls, have been plotted in Fig. 10. It can be seen that the bending angle is practically the same for all the configurations, regardless of the amount of balls. The bending behaviour seems to slow down over time, this is consistent with the expansion rate seen in Fig. 5. This makes sense since the bending and expansion have a direct correlation. The bigger the expansion of the hydrogel particles, the greater the bending.

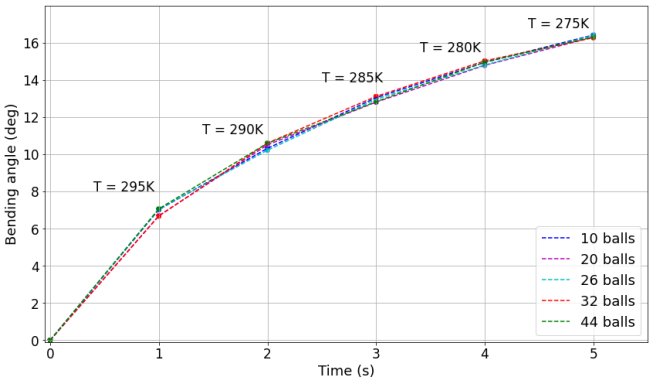

Fig. 10: Bending angle plotted against the time

To find the correlation between the expansion and bending, these two have been plotted against each other in Fig. 11 with the specific bending angle on the vertical axis and the dimensionless diameter on the horizontal axis. The dimensionless diameter is the difference between the current and original diameter, D-D_0, divided by the original diameter, D_0. This gives a better impression of the expansion regardless of the original diameter of the ball. By adding a fitting curve for these five points, a seemingly linear relation can be found with the corresponding equation given in the legend of the graph. This is not surprising since the expansion has a direct impact on the bending angle. The R^2 value of 0.998 has been added to show the accuracy of the curve found, meaning that approximately 99.8% of the observed variation can be explained by the model's inputs.

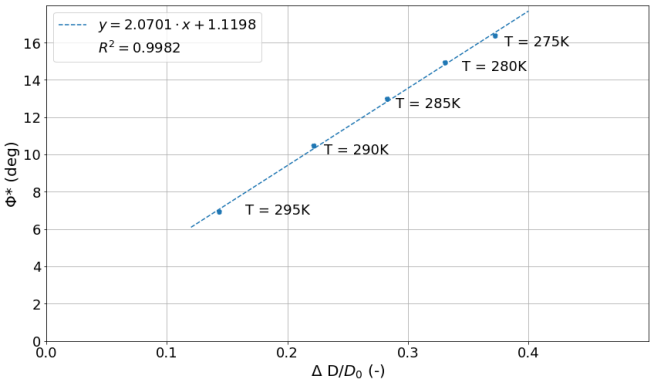

Fig. 11: Bending angle plotted against the deformation

2) C2 - Twists: For the two different alterations, the same bending behaviour found in the C1 cases in one direction, could be found here with an alternating bending angle depending on the material configuration as can be seen in Fig. 12a and Fig. 12b. One important thing to note is that even though the material was slightly stretched the connection with the neighbouring balls stayed intact. This means that curvature in multiple directions was possible without destroying the bonds after an alteration. Furthermore, it can be observed that more bending was obtained by having

more particles in the same material orientation. For example, in Fig. 12b the 'amplitude' is much smaller than in Fig. 12a even though both simulations made use of the same amount of particles.

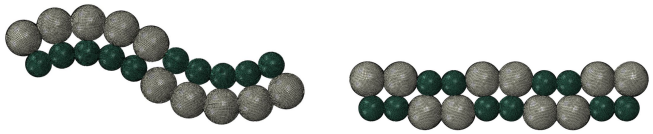

(a) Configuration 2a (b) Configuration 2b

Fig. 12: Configurations with alterations at T = 275K

3) C3 - Hook: For this configuration, a hook shaped configuration was the outcome, this was the first combined configuration with a different number of particles in each sub-configuration. Fig. 13 shows how the entire structure hinged during the expansion of the hydrogel particles in the simulation, with stage 4 being the final form. The hinge point is again the fixed silicone particle on the left corner. The entire structure rotated approximately 240 degrees, which was probably due to the energy involved with the expansion but cannot be explained at this point in time based on the simulations performed within this research scope. However, this is the first configuration with an asymmetric bending pattern this might be the cause for the rotation around the hinge point.

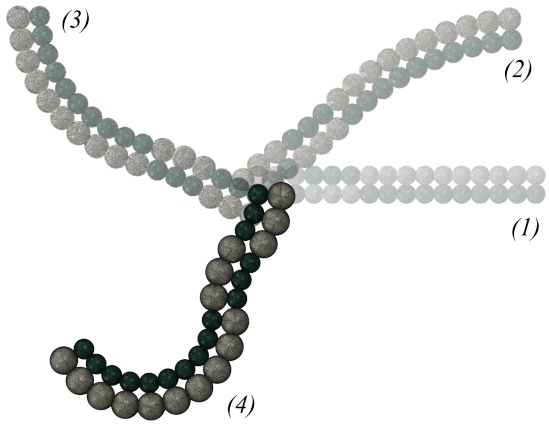

Fig. 13: C3: 'The hook'

4) C4 - Gripper: The following structure resembles a gripper the most by making use of four fingers. The fingers were curling due to the expansion of the hydrogel, resembling a simple gripper. By looking at Fig. 14, it is clear that the structure resembles a horizontal gripper. On the inside, a spherical confinement can be seen due to the curling of four parts. On purpose it was chosen not to have a fully closed gripper due to the absence of interaction constraints the particles would move through each other. However, by leaving the opening in the middle, it clearly functions as a gripper.

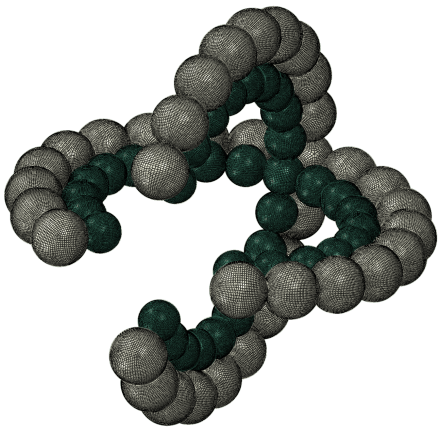

Fig. 14: C4: 'The gripper'

V. CONCLUSIONS

In summary, a model has been built to simulate different configurations which can be potentially used in a soft gripper. This model used the material properties of stimuli-responsive hydrogel and different configurations with temperature as the input factor. Mechanical properties such as expansion and bending angles were the direct output of these models.

The granular structures can be designed with different configurations used in this research to achieve gripping behaviour, this can be further tailored to the required configuration by combining configurations. However, the interaction between the gripper and the external environment should be added to the simulation model. It is clear that the orientation of the materials determines the orientation such as symmetry and the boundary condition. The longer the chain of particles used the longer the simulation run time is. When making a geometry which will deform in three dimensions such as the gripper the run time will increase significantly.

The maximum diameter to be found for a hydrogel ball at T = 275 K is 27.45 mm, which results in a 7.45 mm increase in diameter. This is an expansion of a factor of 1.37 in diameter and a factor of 2.59 in volume. The maximum bending angle between two pairs, ϕ*, is found to be 16.43 degrees at T = 275 K. The bending angle is similar for the configurations with 20, 26, 32 and 44 balls, due to this it can be concluded that the specific bending angle is not dependent on the amount of particles in the first configuration.

In the future, other types of hydrogel can be looked into for different expanding behaviours. In real life, hydrogel particles may not be perfectly spherical. They can have irregular shapes, which affect their expansion and interactions with surrounding materials, leading to different deformation. For further research, geometry differences can be further researched. In addition, other deformation modes besides bending can be explored, such as elongation or twisting. How various structures and materials interact can also be examined to comprehend the contact behaviour between differently shaped structures and materials. This understanding can facilitate the development and utilization of multi-layer or multi-material structures for various applications.

ACKNOWLEDGMENT

This work is financially supported by Delft University of Technology. In addition, thanks for the support from the IWS 3D printing workshop and experiments lab in the Faculty of Mechanical Engineering, Delft University of Technology.

REFERENCES

[1] B. Zhang, Y. Xie, J. Zhou, K. Wang, and Z. Zhang, "State-of-the-art robotic grippers, grasping and control strategies, as well as their applications in agricultural robots: A review," *Computers and Electronics in Agriculture*, vol. 177, p. 105694, 2020. [Online]. Available: https://www.sciencedirect.com/science/article/pii/S0168169920311030

[2] C. Majidi, "Soft robotics: a perspective—current trends and prospects for the future," *Soft robotics*, vol. 1, no. 1, pp. 5–11, 2014.

[3] J. Zhou, S. Chen, and Z. Wang, "A soft-robotic gripper with enhanced object adaptation and grasping reliability," *IEEE Robotics and Automation Letters*, vol. 2, no. 4, pp. 2287–2293, 2017.

[4] M. Manti, T. Hassan, G. Passetti, N. D'Elia, C. Laschi, and M. Cianchetti, "A bioinspired soft robotic gripper for adaptable and effective grasping," *Soft Robotics*, vol. 2, no. 3, pp. 107–116, 2015.

[5] R. Huang, S. Zheng, Z. Liu, and T. Y. Ng, "Recent advances of the constitutive models of smart materials—hydrogels and shape memory polymers," *International Journal of Applied Mechanics*, vol. 12, no. 02, p. 2050014, 2020.

[6] W. Guo, M. Li, and J. Zhou, "Modeling programmable deformation of self-folding all-polymer structures with temperature-sensitive hydrogels," *Smart Materials and Structures*, vol. 22, no. 11, p. 115028, 2013.

[7] Z. Liu, W. Toh, and T. Y. Ng, "Advances in mechanics of soft materials: A review of large deformation behavior of hydrogels," *International Journal of Applied Mechanics*, vol. 7, no. 05, p. 1530001, 2015.

[8] J. Zhang, W. Huang, H. Lu, and L. Sun, "Thermo-/chemo-responsive shape memory/change effect in a hydrogel and its composites," *Materials & Design*, vol. 53, pp. 1077–1088, 2014.

[9] Y. Chen, Y. Zhang, H. Li, J. Shen, F. Zhang, J. He, J. Lin, B. Wang, S. Niu, Z. Han *et al.*, "Bioinspired hydrogel actuator for soft robotics: Opportunity and challenges," *Nano Today*, vol. 49, p. 101764, 2023.

[10] N. Park and J. Kim, "Hydrogel-based artificial muscles: overview and recent progress," *Advanced Intelligent Systems*, vol. 2, no. 4, p. 1900135, 2020.

[11] P. Calvert, "Hydrogels for soft machines," *Advanced Materials*, vol. 21, no. 7, pp. 743–756, 2009. [Online]. Available: https://onlinelibrary.wiley.com/doi/abs/10.1002/adma.200800534

[12] W. Hong, Z. Liu, and Z. Suo, "Inhomogeneous swelling of a gel in equilibrium with a solvent and mechanical load," *International Journal of Solids and Structures*, vol. 46, no. 17, pp. 3282–3289, 2009. [Online]. Available: https://www.sciencedirect.com/science/article/pii/S0020768309001899

[13] J. Zhang, X. Zhao, Z. Suo, and H. Jiang, "A finite element method for transient analysis of concurrent large deformation and mass transport in gels," *Journal of Applied Physics*, vol. 105, no. 9, p. 093522, 2009. [Online]. Available: https://doi.org/10.1063/1.3106628

[14] M. K. Kang and R. Huang, "Swell-induced surface instability of confined hydrogel layers on substrates," *Journal of the Mechanics and Physics of Solids*, vol. 58, no. 10, pp. 1582–1598, 2010. [Online]. Available: https://www.sciencedirect.com/science/article/pii/S0022509610001377

[15] K. K. Westbrook and H. J. Qi, "Actuator designs using environmentally responsive hydrogels," *Journal of Intelligent Material Systems and Structures*, vol. 19, no. 5, pp. 597–607, 2008. [Online]. Available: https://doi.org/10.1177/1045389X07077856

[16] W. Hong, X. Zhao, J. Zhou, and Z. Suo, "A theory of coupled diffusion and large deformation in polymeric gels," *Journal of the Mechanics and Physics of Solids*, vol. 56, no. 5, pp. 1779–1793, 2008. [Online]. Available: https://www.sciencedirect.com/science/article/pii/S0022509607002244

[17] S. Cai and Z. Suo, "Mechanics and chemical thermodynamics of phase transition in temperature-sensitive hydrogels," *Journal of the Mechanics and Physics of Solids*, vol. 59, no. 11, pp. 2259–2278, 2011. [Online]. Available: https://www.sciencedirect.com/science/article/pii/S0022509611001670

[18] Dassault Systèmes, "Abaqus/cae," 2023. [Online]. Available: https://www.3ds.com/products-services/simulia/products/abaqus/abaqus cae/

[19] Q. Chen, D. Schott, and J. Jovanova, "Model-based design of variable stiffness soft gripper actuated by smart hydrogels," *Soft Robotics*, 2024 (Accepted).

[20] F. G. Downs, D. J. Lunn, M. J. Booth, J. B. Sauer, W. J. Ramsay, R. G. Klemperer, C. J. Hawker, and H. Bayley, "Multi-responsive hydrogel structures from patterned droplet networks," *Nature chemistry*, vol. 12, no. 4, pp. 363–371, 2020.

[21] AMT Composites., "Ecoflex 00-10," March 2006. [Online]. Available: https://www.amtcomposites.co.za/product/ecoflex-00-10-0-9kg/

[22] ABAQUS, Inc., "Element library: overview," March 2006. [Online]. Available: https://classes.engineering.wustl.edu/2009/spring/mase5513/abaqus/docs/v6.6/books/usb/default.htm?startat=pt06ch21s01abo21.html